

Application of Splines of the Seventh Order Approximation to the Solution of the Fredholm Integral Equations with Weekly Singularity

I. G. BUROVA, G. O. ALCYBEEV

Department of Computational Mathematics,
St. Petersburg State University,
7-9 Universitetskaya Embankment, St.Petersburg,
RUSSIA

Abstract: - We consider the construction of a numerical solution to the Fredholm integral equation of the second kind with weekly singularity using polynomial spline approximations of the seventh order of approximation. The support of the basis spline of the seventh order of approximation occupies seven grid intervals. In the beginning, in the middle, and at the end of the integration interval, we apply various modifications of the basis splines of the seventh order of approximation. We use the Gaussian-type quadrature formulas to calculate the integrals with a weekly singularity. It is assumed that the solution of the integral equation is sufficiently smooth. The advantages of using splines of the seventh order of approximation include the use of a small number of grid nodes to achieve the required error of approximation. Numerical examples of the application of spline approximations of the seventh order to solve integral equations are given.

Key-Words: - Fredholm integral equation, weekly singularity, polynomial spline approximations.

Received: November 11, 2022. Revised: May 10, 2023. Accepted: June 2, 2023. Published: June 28, 2023.

1 Introduction

As noted in the paper, [1], “Many fields in the area of applied mathematics rely on the knowledge of integral equations, as they arise naturally in various applications in mathematics, engineering, physics, and technology. They can be used to model a wide range of physical problems such as heat conduction, diffusion, continuum mechanics, geophysics, electricity, magnetism, neutron transport, traffic theory, and many more. Integral equations provide solutions to design efficient parametrization algorithms for algebraic curves, surfaces, and hypersurfaces. Many initial and boundary value problems associated with ordinary and partial differential equations can be reformulated as integral equations.

Nowadays, many papers are devoted to the numerical solution of integral equations. We note several papers on this subject.

[1], presents a numerical iterative method for the approximate solutions of nonlinear Volterra integral equations of the second kind, with weekly singular kernels. The author of the paper derives conditions so that a unique solution of such equations exists as the unique fixed point of an integral operator. The iterative application of that operator to an initial function yields a sequence of functions converging to the true solution. Finally, an appropriate numerical integration scheme (a certain type of

product integration) is used to produce the approximations of the solution at given nodes.

In the paper, [2], a computational scheme is presented to solve weakly singular integral equations of the second kind. The discrete collocation method in addition to the moving least squares (MLS) technique established on scattered points is utilized to estimate the solution of integral equations. The discrete collocation technique for the approximate solution of integral equations results from the numerical integration of all integrals in the method. The authors utilize an accurate quadrature formula based on the use of the nonuniform composite Gauss-Legendre integration rule and employ it to compute the singular integrals which appeared in the approach.

In the paper, [3], product integration methods based on discrete spline quasi-interpolants and application to weakly singular integral equations are presented.

In paper, [4], the advanced multistep and hybrid methods have been used to solve the Volterra integral equation.

In paper, [5], the kernel was initially approximated through the Legendre wavelet functions.

In paper, [6], the forward-jumping methods of the hybrid type are used for the construction of the methods with a high order of accuracy.

In the paper, [7], the Fourier integral transform has been employed to reduce the problem of determining the stress component under the contact region of a punch in solving dual integral equations.

In the paper, [8], the method of integral equations is proposed for some of the electrical engineering problems (current density, heat conduction). The presented models lead to a system of Fredholm integral equations, integro-differential equations, or Volterra-Fredholm integral equations, respectively.

[9], presents the thermal desorption functional differential equations of the neutral type with integrable weak singularity.

The purpose of the paper, [10], is to investigate the design of the skin surface electrodes for functional electrical stimulation using an isotropic single-layered model of the skin and underlying tissue. It is shown that the electric potential satisfies a weakly singular Fredholm integral equation of the second kind.

In the paper, [11], the Newton-iteration scheme based on the Galerkin and the multi-Galerkin operators is constructed. It can be used to solve non-linear integral equations of the Fredholm-Hammerstein type for both smooth and weakly singular algebraic kernels.

In the paper, [12], a new computational method that is based on a special B-spline is provided.

Previously, the authors constructed a solution to integral equations with a weak singularity using splines of the second order of approximation, [13].

In the present paper, the solutions of the integral equations of the second kind with a weak singularity are constructed using the splines of the seventh order of approximation. In addition, a comparison is made with the results of using splines of the second order of approximation.

2 Problem Formulation

We discuss the numerical solution of the integral equation of the second kind

$$(Au)(x) \equiv u(x) - \int_a^b g(x,s)K(x,s)u(s)ds = q(x),$$

$x \in [a, b]$, where $g(x, s) = \frac{1}{|x-s|^\alpha}$, $\alpha \in (0,1)$.

We assume that $K(x, s)$ and the right side of the equation $q(x)$ are continuous. In addition, we assume that the equation is uniquely solvable and the estimate for the norm of the inverse operator in space C is known: $\|A^{-1}\| \leq B$.

First, consider the approximation properties of polynomial splines of the seventh order of

approximation. Let $\{x_i\}$ be a uniform grid of nodes on the interval $[a, b]$: $a = x_0 < \dots < x_n = b$ with step h . Let us assume that the values of the function $u(x)$ are given at the grid nodes.

Let r, r_1 be integers, $r + r_1 = 7$, $r \geq 1, r_1 \geq 1$, and the spline ω_k be such that $\text{supp } \omega_k = [x_{k-r}, x_{k+r_1}]$. The approximation using basis splines is built separately on each grid interval. This approximation is constructed in the form of the sum of the products of the values of the function u at the grid nodes and the basis splines $\omega_j(x)$. Following the methodology developed by Professor S. G. Mikhlin, we find the basic functions ω_k by solving the system of approximation relations

$$\sum_{j=k-r_1+1}^{k+r} x_j^s \omega_j(x) = x^s, \quad x \in [x_k, x_{k+1}],$$

$$s = 0, 1, \dots, 6. \quad (1)$$

With different values of the parameters r, r_1 , we get basis splines suitable for approximation at the different parts of the interpolation interval $[a, b]$. At the beginning of the interpolation interval $[a, b]$ we use the right basis splines ω_j^R . In the middle of the interpolation interval $[a, b]$ we use the middle basis splines ω_j^M . At the end of the interpolation interval $[a, b]$ we use the left basis splines ω_j^L .

2.1 Approximation Theorem

Further, we will use the norm of the vector of the form:

$$\|u\|_{C[a,b]} = \max_{x \in [a,b]} |u(x)|.$$

Consider the approximation with the right basis splines. Let $r_1 = 1, r = 6$, in this case, on the interval $[x_k, x_{k+1}]$ the formula for the right spline takes the form:

$$\tilde{u}(x) = \sum_{j=k}^{k+6} u(x_j) \omega_j^R(x), \quad x \in [x_k, x_{k+1}],$$

where the right basis splines $\omega_j^R(x)$ have the form:

$$\omega_k^R(x) = \frac{c_k(x)}{d_k},$$

$$c_k(x) = (x - x_{k+6})(x - x_{k+5})(x - x_{k+4}) \times (x - x_{k+3})(x - x_{k+2})(x - x_{k+1}),$$

$$d_k = (x_k - x_{k+6})(x_k - x_{k+5})(x_k - x_{k+4}) \times (x_k - x_{k+3})(x_k - x_{k+2})(x_k - x_{k+1});$$

$$\omega_{k+1}^R(x) = \frac{c_{k+1}(x)}{d_{k+1}},$$

$$c_{k+1}(x) = (x - x_{k+6})(x - x_{k+5})(x - x_{k+4}) \times (x - x_{k+3})(x - x_{k+2})(x - x_k),$$

$$d_{k+1} = (x_{k+1} - x_{k+6})(x_{k+1} - x_{k+5})$$

$$\begin{aligned} &\times (x_{k+1} - x_{k+4})(x_{k+1} - x_{k+3}) \\ &\times (x_{k+1} - x_{k+2})(x_{k+1} - x_k); \end{aligned}$$

$$\omega_{k+2}^R(x) = \frac{c_{k+2}(x)}{d_{k+2}},$$

$$\begin{aligned} c_{k+2}(x) &= (x - x_{k+6})(x - x_{k+5})(x - x_{k+4}) \\ &\times (x - x_{k+3})(x - x_{k+1})(x - x_k), \\ d_{k+2} &= (x_{k+2} - x_{k+6})(x_{k+2} - x_{k+5}) \\ &\times (x_{k+2} - x_{k+4})(x_{k+2} - x_{k+3}) \\ &\times (x_{k+2} - x_{k+1})(x_{k+2} - x_k); \end{aligned}$$

$$\omega_{k+3}^R(x) = \frac{c_{k+3}(x)}{d_{k+3}},$$

$$\begin{aligned} c_{k+3}(x) &= (x - x_{k+6})(x - x_{k+5})(x - x_{k+4}) \\ &\times (x - x_{k+2})(x - x_{k+1})(x - x_k), \\ d_{k+3} &= (x_{k+3} - x_{k+6})(x_{k+3} - x_{k+5}) \\ &\times (x_{k+3} - x_{k+4})(x_{k+3} - x_{k+2}) \\ &\times (x_{k+3} - x_{k+1})(x_{k+3} - x_k); \end{aligned}$$

$$\omega_{k+4}^R(x) = \frac{c_{k+4}(x)}{d_{k+4}},$$

$$\begin{aligned} c_{k+4}(x) &= (x - x_{k+6})(x - x_{k+5})(x - x_{k+3}) \\ &\times (x - x_{k+2})(x - x_{k+1})(x - x_k), \\ d_{k+4} &= (x_{k+4} - x_{k+6})(x_{k+4} - x_{k+5}) \\ &\times (x_{k+4} - x_{k+3})(x_{k+4} - x_{k+2}) \\ &\times (x_{k+4} - x_{k+1})(x_{k+4} - x_k); \end{aligned}$$

$$\omega_{k+5}^R(x) = \frac{c_{k+5}(x)}{d_{k+5}},$$

$$\begin{aligned} c_{k+5}(x) &= (x - x_{k+6})(x - x_{k+4})(x - x_{k+3}) \\ &\times (x - x_{k+2})(x - x_{k+1})(x - x_k), \\ d_{k+5} &= (x_{k+5} - x_{k+6})(x_{k+5} - x_{k+4}) \\ &\times (x_{k+5} - x_{k+3})(x_{k+5} - x_{k+2}) \\ &\times (x_{k+5} - x_{k+1})(x_{k+5} - x_k); \end{aligned}$$

$$\omega_{k+6}^R(x) = \frac{c_{k+6}(x)}{d_{k+6}},$$

$$\begin{aligned} c_{k+6}(x) &= (x - x_{k+5})(x - x_{k+4})(x - x_{k+3}) \\ &\times (x - x_{k+2})(x - x_{k+1})(x - x_k), \\ d_{k+6} &= (x_{k+6} - x_{k+5})(x_{k+6} - x_{k+4}) \\ &\times (x_{k+6} - x_{k+3})(x_{k+6} - x_{k+2}) \\ &\times (x_{k+6} - x_{k+1})(x_{k+6} - x_k). \end{aligned}$$

Formulas for the left and the middle splines can be found in paper, [14]. When approximating a function with the splines of the 7th order of approximation, the next Theorem is valid.

Theorem. If $\text{supp } \omega_k = [x_{k-1}, x_{k+6}]$, then we have the left splines. The following inequalities are valid:

$$\begin{aligned} |u(x) - \tilde{u}(x)|_{x \in [x_k, x_{k+1}]} \\ \leq 95.842 \cdot h^7 \frac{\|u^{(7)}\|_{C[x_{k-5}, x_{k+1}]}}{7!}. \end{aligned}$$

If $\text{supp } \omega_k = [x_{k-3}, x_{k+4}]$, then we have the middle splines. The following approximation estimate is valid:

$$\begin{aligned} |u(x) - \tilde{u}(x)|_{x \in [x_k, x_{k+1}]} &\leq 12.359 \cdot \\ &h^7 \frac{\|u^{(7)}\|_{C[x_{k-3}, x_{k+3}]}}{7!}. \end{aligned}$$

If $\text{supp } \omega_k = [x_{k-6}, x_{k+1}]$, then we have the right splines. The following approximation estimate is valid:

$$\begin{aligned} |u(x) - \tilde{u}(x)|_{x \in [x_k, x_{k+1}]} \\ \leq 95.842 \cdot h^7 \frac{\|u^{(7)}\|_{C[x_k, x_{k+6}]}}{7!}. \end{aligned}$$

Proof. In the case of approximating the function u on the interval $[x_k, x_{k+1}]$ near the left end of the interval $[a, b]$, we use the right basis splines:

$$\tilde{u}(x) = \sum_{j=k}^{k+6} u(x_j) \omega_j^R(x) dx, \quad x \in [x_k, x_{k+1}].$$

Let us estimate the approximation error on the interval $[x_k, x_{k+1}]$ when the right basis splines were used. Using the formula of the remainder term of the interpolation polynomial that solves the Lagrange interpolation problem, we obtain the relation

$$\begin{aligned} u(x) - \tilde{u}(x) &= \frac{u^{(7)}(\xi)}{7!} (x - x_k) \dots (x - x_{k+6}), \\ &\xi \in [x_k, x_{k+6}]. \end{aligned}$$

There is a product $(x - x_k) \dots (x - x_{k+6})$ in the error estimate. Let the ordered grid of nodes $\{x_k\}$ be uniform with step h . Let us estimate the product of factors $(x - x_k) \dots (x - x_{k+6})$. Thus, estimating the maximum of the expression $\frac{u^{(7)}(\xi)}{7!} (x - x_k) \dots (x - x_{k+6})$, where $\xi \in [x_k, x_{k+6}]$, we obtain $\|u(x) - \tilde{u}(x)\|_{C[x_k, x_{k+1}]} \leq Kh^7 \|u^{(7)}\|_{C[x_k, x_{k+6}]}$. Similarly, we obtain an approximation estimate on the grid interval $[x_k, x_{k+1}]$ with the left and middle splines.

This completes the proof of the theorem.

3 Problem Solution

The application of the local splines of the seventh order of approximation can be applied to calculate integrals with a weekly singularity. First of all, we note how to apply local splines of the seventh order of approximation to calculate integrals over the interval $[a, b]$. As already noted, the spline approximation of the function is applied separately

to each grid interval. Let s_j be the nodes of the set on the interval $[a, b]$:

$$a = s_0 < s_1 < \dots < s_n = b, n \geq 10.$$

We represent the integral in the form:

$$\int_a^b g(x, s)K(x, s)u(s)ds = \sum_{k=0}^{n-1} \int_{s_k}^{s_{k+1}} g(x, s)K(x, s)u(s)ds,$$

where $g(x, s) = \frac{1}{|x-s|^\alpha}, \alpha \in (0, 1)$.

The function $f(s) = K(x, s)u(s), s \in [s_k, s_{k+1}]$ can be approximated with the expression: $f(s) \approx \tilde{f}(s) = K(x, s)\tilde{u}(s)$. Let us denote $c_j \approx u(s_j)$.

Thus we obtain

$$u(x) - \sum_{k=0}^2 \sum_{j=k}^{k+6} c_j \int_{s_k}^{s_{k+1}} K(x, s)\omega_j^R(s)ds + \sum_{k=3}^{n-4} \sum_{j=k-3}^{k+3} c_j \int_{s_k}^{s_{k+1}} K(x, s)\omega_j^M(s)ds + \sum_{k=n-3}^{n-1} \sum_{j=n-3}^{n-1} c_j \int_{s_k}^{s_{k+1}} K(x, s)\omega_j^L(s)ds = g(x).$$

Now we have to solve the system of equations

$$c_i - \sum_{k=0}^2 \sum_{j=k}^{k+6} c_j \int_{s_k}^{s_{k+1}} K(x_i, s)\omega_j^R(s)ds + \sum_{k=3}^{n-4} \sum_{j=k-3}^{k+3} c_j \int_{s_k}^{s_{k+1}} K(x_i, s)\omega_j^M(s)ds + \sum_{k=n-3}^{n-1} \sum_{j=n-3}^{n-1} c_j \int_{s_k}^{s_{k+1}} K(x_i, s)\omega_j^L(s)ds = g(x_i),$$

$$i = 0, \dots, n - 1.$$

We assume that the integrals

$$\int_{s_k}^{s_{k+1}} K(x_i, s)\omega_j^R(s)ds, \int_{s_k}^{s_{k+1}} K(x_i, s)\omega_j^M(s)ds, \int_{s_k}^{s_{k+1}} K(x_i, s)\omega_j^L(s)ds,$$

can be computed exactly. Otherwise, we can use the quadrature formulas. In this case, it is necessary to take into account the error of the applied quadrature formulas. When solving integral equations, local polynomial splines give an acceptable solution with a small number of operations and in a short time. If the integral has a weight function, then we can use the Gaussian type's quadrature formulas. In this case, we separate the singularity into a weight function. It is possible to use Gaussian-type composite quadrature formulas on the interval $[x_k, x_{k+1}]$ by applying a Gaussian-type formula with one node on each subinterval. However, the result will be better if, on each

interval, a Gaussian-type formula with four nodes is applied.

4 Numerical Examples

Example 1. Consider the following integral equation from paper, [3]:

$$u(t) - \int_0^1 |t - s|^{-\frac{1}{2}} u(s)ds = q(t), t \in [0, 1],$$

where $q(t)$ is chosen such that the exact solution is $u(t) = \exp(t)$. Fig. 1 shows the graph of the right side of the equation. On the interval $[0, 1]$ we construct a uniform grid of nodes with the step $h = \frac{1}{n}$. Using splines of the seventh order of approximation, we construct the system of equations. Note that in numerical calculations of integrals with a weakly singularity, we can use the Gaussian-type formulas with three or four nodes over the interval $[x_k, x_{k+1}]$.

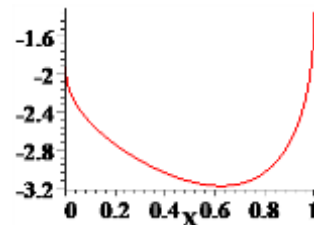


Fig 1: The plot of the function $q(t)$.

Calculations are made in the MAPLE system with $Digits = 15$. Fig. 2, Fig. 3, Fig. 4, and Fig. 5 show graphs of the solution errors in absolute value for different numbers of grid nodes. Fig.2 shows the plot of the errors obtained with the polynomial splines of the second-order approximation (with 16 nodes), [13]. Note, that the numbers of the grid nodes are marked along the abscissa axis. Fig.3 shows the plot of the errors obtained with the polynomial splines of the seventh-order approximation (with 10 nodes). Fig. 4 shows the plot of the errors obtained with the polynomial splines of the seventh-order approximation (with 32 nodes). Fig. 5 shows the plot of the errors obtained with the polynomial splines of the second-order approximation (with 32 nodes).

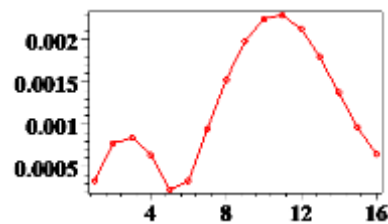


Fig. 2: The plot of the errors obtained with the polynomial splines of the second-order approximation (16 nodes).

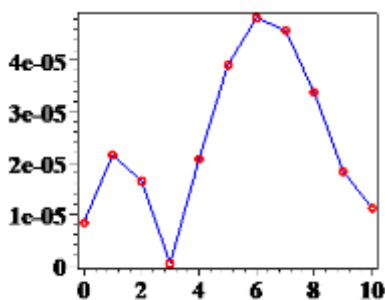


Fig. 3: The plot of the obtained errors with the polynomial splines of the seventh order (10 nodes).

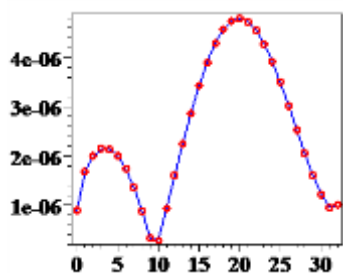


Fig. 4: The plot of the obtained errors with the polynomial splines of the seventh-order approximation (32 nodes).

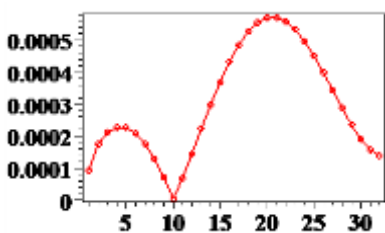


Fig 5: The plot of the obtained errors with the second-order polynomial splines (32 nodes).

Example 2. Consider the following integral equation from the paper, [3]:

$$u(t) - \int_0^\pi \sin(s-t)|t-s|^{-\frac{1}{2}}u(s)ds = f(t),$$

$t \in [0, \pi]$, where $f(t)$ is chosen such that the exact solution is $u(t) = \cos(t)$.

The plot of the function $f(t)$ is given in Fig.6.



Fig. 6: The plot of the function $f(t)$.

We construct a uniform grid of nodes with the step, $h = \frac{1}{n}$. Using splines of the seventh order of approximation, we construct the system of

equations. Fig. 7, Fig. 8, Fig. 9, Fig. 10, and Fig. 11 show graphs of the solution errors in absolute value for different numbers of grid nodes. Fig. 7 shows the plot of the errors obtained with the polynomial splines of the second-order approximation (with 64 nodes). Fig.8. shows the plot of the errors obtained with the polynomial splines of the second-order approximation (with 16 nodes). Fig. 9 shows the plot of the errors obtained with the polynomial splines of the second-order approximation (with 32 nodes). Fig. 10 and Fig. 11 show the plot of the errors obtained with the polynomial splines of the seventh-order approximation (with 32 and 16 nodes). Calculations are made in the MAPLE system with $Digits = 15$.

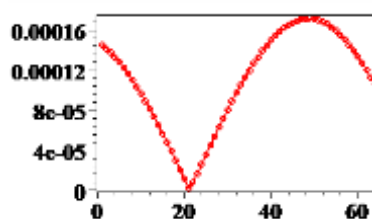


Fig. 7: The plot of the obtained errors with the polynomial splines of the second-order approximation (64 nodes).

Note that in numerical calculations of integrals with a weak singularity, we can use Gaussian-type formulas with three or four nodes over the interval $[x_k, x_{k+1}]$, or composite Gaussian-type quadrature formulas. For example, when $n = 16$, the division into 128 subintervals was used, and in the case of $n = 32$, the division into 256 subintervals was used. On every subinterval, one node was taken. The results are shown in Fig.10 and Fig. 11. Calculations are made in the MAPLE system with $Digits = 15$.

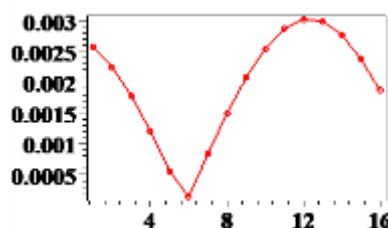


Fig. 8: The plot of the obtained errors with the polynomial splines of the second order (16 nodes).

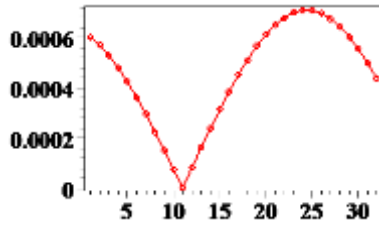


Fig. 9: The plot of the obtained errors with the polynomial splines of the second-order approximation (32 nodes).

Note that in numerical calculations of integrals with a weak singularity, we can use the Gaussian-type formulas with three or four nodes over the interval, $[x_k, x_{k+1}]$, or composite Gaussian-type quadrature formulas. For example, when $n = 16$, the division into 128 subintervals was used, and in the case of $n = 32$, the division into 256 subintervals was used. On every subinterval, one node was taken. The results are shown in Fig. 10 and Fig. 11. Calculations are made in the MAPLE system with *Digits* = 15. Fig. 12 shows a graph of the solution error when the Gaussian-type formula with four nodes was applied on every grid interval $[x_k, x_{k+1}]$ and $n = 64$. We get the maxima error in absolute value which equals to $0.2 \cdot 10^{-12}$. Calculations are made in the MAPLE system with *Digits* = 20.

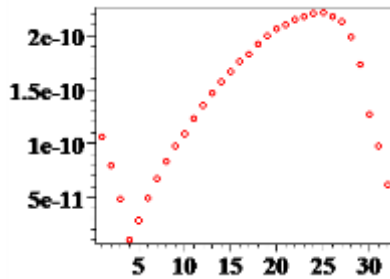


Fig. 10: The plot of the obtained errors with the polynomial splines of the seventh order (32 nodes).

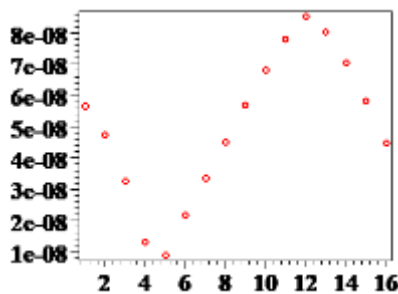


Fig. 11: The plot of the obtained errors with the polynomial splines of the seventh order (16 nodes).

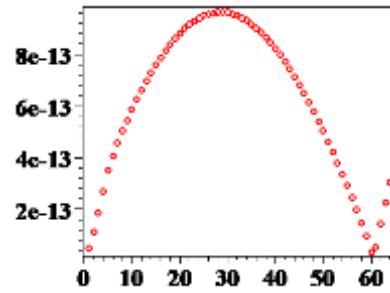


Fig. 12: The plot of the obtained errors with the polynomial splines of the seventh order (64 nodes).

Let u^* be the exact solution and u^h the approximate solution of the integral equation. Table 1 shows the maxima errors in absolute value ($\|u^* - u^h\|_\infty$).

The errors obtained using splines of the second order of approximation are given in the second column in Table 1. The errors obtained using splines of the seventh order of approximation are given in the third column in Table 1. The last column in Table 1 contains the result from Paper, [3]. The first column contains the number of nodes n . In Table 1, the error of the solution was calculated when the composite quadrature Gauss type's formula with four nodes on every grid interval $[x_k, x_{k+1}]$ was applied in the case of splines of the seventh order of approximation. Note that the values of the solution error presented in Table 1 correspond to the theoretical errors of approximation with the corresponding splines of the second or the seventh order of approximation.

Table 1. The maxima errors in absolute value

n	The maxima errors in absolute value		
	<i>Splines of the 2nd order of approximation</i>	<i>Splines of the 7th order of approximation</i>	<i>Results from paper, [3]</i>
16	$0.3 \cdot 10^{-2}$	$0.4 \cdot 10^{-7}$	$0.4 \cdot 10^{-3}$
32	$0.6 \cdot 10^{-3}$	$0.2 \cdot 10^{-9}$	$0.4 \cdot 10^{-4}$

4 Conclusion

In this paper, we present a numerical scheme to solve the Fredholm equation of the second kind with a weak singularity. This scheme can be used for engineering calculations. If we compare numerical methods based on local spline approximations of different orders of accuracy, we note the following. Numerical methods based on the local spline approximations of the seventh order of approximation, give a more accurate result when the solution is sufficiently smooth. In this case, we can use a small number of grid nodes. The advantages of

using splines of the seventh order of approximation include the use of a small number of grid nodes to achieve the required error of approximation.

In the following papers, a generalization will be made to the case of a solution from several variables.

Acknowledgment:

The authors are gratefully indebted to St. Petersburg University for their financial support in the preparation of this paper (Pure ID 104625746), as well as to a resource center for providing the package Maple.

References:

- [1] S. Micula, A Numerical Method for Weakly Singular Nonlinear Volterra Integral Equations of the Second Kind, *Symmetry*, Vol. 2020, 1862.
- [2] P. Assari, Solving Weakly Singular Integral Equations utilizing the Meshless Local discrete Collocation Technique, *Alexandria Engineering Journal*, Vol. 57, No 4, December 2018, pp. 2497-2507.
- [3] C. Allouch, P. Sablonnière, D. Sbibiha, M. Tahrichi, Product Integration Methods based on Discrete Spline Quasi-interpolants and Application to Weakly Singular Integral Equations, *Journal of Computational and Applied Mathematics*, Vol. 233, 2010, pp. 2855–2866.
- [4] M. Galina., I. Vagif, I. Mehriban, On the Construction of the Advanced Hybrid Methods and Application to solving Volterra Integral Equation, *WSEAS Transactions on Systems and Control*, Vol. 14, 2019, pp. 183-189.
- [5] S. Rahbar, Solving Fredholm Integral Equation using Legendre Wavelet Functions, *WSEAS Transactions on Mathematics*, No. 3, 2004, pp. 591-595.
- [6] M. Galina, I. Vagif, I. Mehriban, On the Construction of the Forward-Jumping Method and its Application to Solving of the Volterra Integral Equations with Symmetric Boundaries, *WSEAS Transactions on Mathematics*, Vol. 16, 2017, pp. 295-302.
- [7] S. Saha, V. Kumar, A. N. Das, An Elastic Half Space with a Moving Punch, *WSEAS Transactions on Applied and Theoretical Mechanics*, Vol. 16, 2021, pp. 245-249.
- [8] L. Hącia, K. Bednarek, A. Tomczewski, Computational Results for Integral Modeling in Some Problems of Electrical Engineering, *WSEAS International Conference on Computers*, 2007, pp. 114-119.
- [9] Yury V. Zaika, Ekaterina K. Kostikova, Functional Differential Equations of neutral Type with Integrable Weak Singularity: Hydrogen Thermal Desorption Model, *IOP Conf. Series: Journal of Physics: Conf. Series*, Vol. 929, 2017, doi:10.1088/1742-6596/929/1/012034.
- [10] M. G. Cassar, C. Sebu, M. Pidcock, S. Chandak, B. Andrews, Optimal Design of Electrodes for Functional Electrical Stimulation Applications to Single Layer Isotropic Tissues, *The International Journal for Computation and Mathematics in Electrical and Electronic Engineering*, Vol. 42, No. 3, 2023, pp. 695-707.
- [11] S. Chakraborty, K. Kant, G. Nelakanti, Error Analysis of Reiterated Projection Methods for Hammerstein Integral Equations, *International Journal of Computer Mathematics*, Vol. 99, No. 10, 2022, pp. 2001-2017.
- [12] M. Mohammad, C. Cattani, A Collocation Method via the Quasi-Affine Biorthogonal Systems for Solving Weakly Singular Type of Volterra-Fredholm Integral Equations. *Alexandria Engineering Journal*, Vol. 59, No. 4, 2020, pp. 2181-2191.
- [13] I. G. Burova, G. O. Alcybeev, Solution of Integral Equations Using Local Splines of the Second Order, *WSEAS Transactions on Applied and Theoretical Mechanics*, Vol. 17, 2022, pp. 258-262.
- [14] I. G. Burova, G. O. Alcybeev, The Application of Splines of the Seventh Order Approximation to the Solution of Integral Fredholm Equations, *WSEAS Transactions on Mathematics*, Vol. 22, 2023, pp. 409-418.

Contribution of Individual Authors to the Creation of a Scientific Article (Ghostwriting Policy)

G.O. Alcybeev executed the numerical experiments.

I. G. Burova developed the theoretical part.

Sources of Funding for Research Presented in a Scientific Article or Scientific Article Itself

The authors are gratefully indebted to St. Petersburg University for their financial support in the preparation of this paper (Pure ID 104625746).

Conflict of Interest

The authors have no conflicts of interest to declare that are relevant to the content of this article.

Creative Commons Attribution License 4.0 (Attribution 4.0 International, CC BY 4.0)

This article is published under the terms of the Creative Commons Attribution License 4.0

https://creativecommons.org/licenses/by/4.0/deed.en_US